Next, we wish to investigate the behavior of $C_L^{3/2}/C_D$ for $\xi \neq 0$. The underlying idea for constructing a wider class of lifting surfaces is to use the streamlines of our basic flowfield as the elements of the surface. Then the lifting surface is formed by those streamlines that penetrate the basic shock surface through the points on the leading-edge curve. See Fig. 1. Let us now define the lift and the drag coefficients as functions of ξ:

$$C_{L(\xi)} = -\frac{4}{\gamma+1}\, k^2 a^2 \delta^2 \xi^{2k-1} \int_1^{\frac{\xi}{\xi+1}} \eta^{-\frac{2}{\gamma+1}} R(\eta)\, d\eta \tag{12}$$

The integral in the last equation can be found by using the momentum equation. Hence,

$$C_{L(\xi)} = \frac{4}{\gamma+1}\, k^2 a^2 \delta^2\, \frac{1}{2k-1}\, (\xi+1)^{2k-1} \left(\frac{\xi}{\xi+1}\right)^{2k-\frac{2}{\gamma+1}} \times \left[R\left(\frac{\xi}{\xi+1}\right) - U\left(\frac{\xi}{\xi+1}\right) \right] \tag{13}$$

Similarily, we have for the drag coefficient

$$C_{D(\xi)} = -\frac{8}{(\gamma+1)^2}\, k^3 a^3 \delta^3 \xi^{3k-2} \int_1^{\frac{\xi}{\xi+1}} \eta^{\frac{\gamma-3}{\gamma+1}} R(\eta) U(\eta)\, d\eta \tag{14}$$

Using momentum and continuity, we can integrate and obtain

$$C_{D(\xi)} = -\frac{8}{(\gamma+1)^2} k^3 a^3 \delta^3 \frac{1}{3k-2} (\xi+1)^{3k-2} \left(\frac{\xi}{\xi+1}\right)^{3k-\frac{4}{\gamma+1}} \times \left[U\left(\frac{\xi}{\xi+1}\right) R\left(\frac{\xi}{\xi+1}\right) - \frac{U\left(\frac{\xi}{\xi+1}\right)^2}{2} - \frac{1}{2} R\left(\frac{\xi}{\xi+1}\right)^{\frac{\gamma-1}{\gamma}} \right] \tag{15}$$

Finally, we obtain for the formula for a general two-dimensional waverider

$$\frac{C_{L(\xi)}^{3/2}}{C_{D(\xi)}} = \sqrt{\gamma+1}\, \frac{3k-2}{(2k-1)^{3/2}} \sqrt{\xi+1} \times \frac{\left\{ \eta^{2k-\frac{2}{\gamma+1}} [R(\eta) - U(\eta)] \right\}^{3/2}}{\left\{ \eta^{3k-\frac{4}{\gamma+1}} \left[U(\eta) R(\eta) - \frac{U(\eta)^2}{2} - \frac{1}{2} R(\eta)^{\frac{\gamma-1}{\gamma}} \right] \right\}} \tag{16}$$

at $\eta = \xi/\xi+1$. An examination of the behavior of $C_{L(\xi)}^{3/2}/C_{D(\xi)}$ shows an increase of the maxima as ξ increases whereas the k where the maxima are attained also increase. The highest maximum value of $C_{L(\xi)}^{3/2}/C_{D(\xi)}$ is the limiting case $\xi \to \infty$ and $k_{max} \to \infty$ that corresponds to the body shape supporting exponential shock shapes. The limiting value is $C_{L(\xi)}^{3/2}/C_{D(\xi)} = 1.5795$. This special case was worked out earlier by Cole and Areosty.[7]

Concluding Remarks

Details of above investigations can be found in Wagner.[8] The analysis is part of a study of optimum lifting surfaces using HSDT and will be used, in a subsequent paper, to design three-dimensional waveriders supported by two-dimensional flowfields. This represents a generalization of the idea by Nonweiler[9] to design three-dimensional inverted-V wings supported by the two-dimensional flowfield generated by a flat plate.

Acknowledgments

This work was supported by the Air Force Office of Scientific Research under Grant AFOSR 88-0037. It is my great pleasure to express at this point my gratitude to Julian D. Cole who suggested this problem to me and provided me with very helpful advice and guidance.

References

[1]Cole, J. D., "Newtonian Flow Theory for Slender Bodies," *Journal of the Aeronautical Sciences,* Vol. 24, No. 6, 1957, pp. 448–455.

[2]Mirels, H., "Hypersonic Flow Over Slender Bodies Associated with Power-Law Shocks," *Advances in Applied Mechanics,* Vol. 7, 1962.

[3]Chernyi, G. G., *Introduction to Hypersonic Flow,* Academic, New York, 1961.

[4]Gersten, K., and Nicolai, D., *Die Hyperschallströmung um schlanke Körper mit Konturen der Form* $\bar{R} = \bar{x}^n$, Deutsche Luft- and Raumfahrt Forschungsbericht 64-19, July, 1964.

[5]Sullivan, P. A., "Inviscid Hypersonic Flow on Cusped Concave Surfaces," *Journal of Fluid Mechanics,* Vol. 24, No. 1, 1966.

[6]Cole, J. D., and Aroesty, J., "Optimum Hypersonic Lifting Surfaces Closer to Flat Plates," *AIAA Journal,* Vol. 3, Aug. 1965, pp. 1520–1522.

[7]Cole, J. D., and Aroesty, J., "Hypersonic Similarity Solutions for Airfoils Supporting Exponential Shock Waves," *AIAA Journal,* Vol. 8, No. 2, 1970, pp. 308–315.

[8]Wagner, B. A., "Hypersonic Similarity Solutions for Airfoils Supporting Power Law Shock Waves," Rensselaer Polytechnic Institute, Troy, NY, RPI Math. Rept. 168, July 1988.

[9]Nonweiler, T. R. F., "Delta Wings of Shapes Amenable to Exact Shock Wave Theory," *Journal of the Royal Aeronautical Society,* Vol. 67, No. 625, Jan. 1963.

Effect of Slotting on the Noise of an Axisymmetric Supersonic Jet

Anjaneyulu Krothapalli*
Florida A&M University/Florida State University, Tallahassee, Florida 32316

James McDaniel†
University of Virginia, Charlottesville, Virginia 22903
and
Donald Baganoff‡
Stanford University, Stanford, California 94305

Introduction

THE purpose of this Note is to report the results of an experiment that demonstrates a simple concept for noise reduction in a supersonic jet exiting from a converging axisymmetric nozzle. The basic axisymmetric nozzle exit geometry is modified by the addition of fingers, as shown in Fig. 1.

It is well-known that the structure of a choked underexpanded jet has features different from those of subsonic and ideally expanded supersonic jets. These features include dis-

Received June 22, 1989; revision received Dec. 9, 1989; second revision received Feb. 1, 1990; accepted for publication Feb. 5, 1990.

*Professor and Chairman, Department of Mechanical Engineering, College of Engineering. Member AIAA.

†Associate Professor, Department of Aerospace and Mechanical Engineering. Member AIAA.

‡Professor, Department of Aeronautics and Astronautics. Member AIAA.

crete tones in the sound spectrum, known as screech tones, and the presence of shock cells. The jet screech phenomenon, which is commonly associated with underexpanded jet flows, was described by Powell[1] as arising through a feedback mechanism. The near-sound field and the associated flow structure of a choked jet were well-characterized by a large amount of experimental data available in the literature, and a list of references can be found in a paper by Yu and Seiner.[2] Numerous investigations have been conducted in the past in an attempt to understand the underlying physics of the jet screech and its effects on mixing of the jet. Some investigators have used the acoustic feedback mechanism to alter the mixing and noise characteristics of the underexpanded jet using sound reflectors near the nozzle exit.[3,4] Depending on the position of the reflector, some improved mixing and absence of screech tones were observed. In this work, fingers or slots are added to the base nozzle as a means to provide enhanced mixing of the jet near the nozzle exit.

The principle parameters or variables governing the flow of a free underexpanded axisymmetric jet are the following: the pressure ratio (stagnation pressure / ambient pressure) R, the Mach number M, the Reynolds number Re, and the condition of the flow at the nozzle exit. In the present investigation, the pressure ratio is varied from 2 to 5. This interval corresponds to a Mach number range, based on fully expanded isentropic flow, of 1.05–1.5. The Reynolds number employed here is based on the diameter D, of the nozzle exit and given by $Re = (M \times a \times D)/v$, where a and v are the speed of sound and kinematic viscosity of the ambient medium, respectively. This Reynolds number is varied from 2.4 to 3.4×10^5. The inlet geometry of the nozzle is designed to obtain a low turbulence level at the exit plane of the nozzle. The total pressure profile at the exit plane of the nozzle is found to be quite flat.

Apparatus, Instrumentation, and Procedures

A high pressure, blow-down-type air supply system is used to provide the airflow to the cylindrical settling chamber having dimensions of 1.75 m long and 0.6 m in diameter. To minimize disturbances at the nozzle exit, the air is passed through an adapter before reaching the nozzle, containing six screens, set 5 cm apart. The ratio of areas between the adapter and the nozzle exit is about 40. The plain (unslotted) nozzle is a converging axisymmetric nozzle having an exit diameter of 1 cm. The slotted nozzle is of similar geometry except for the six fingers added to the base nozzle. The length of the fingers is about 1.4 cm (see Fig. 1).

A conventional shadowgraph system is used for flow visualization purposes. For downstream distances less than 15 diam, where the velocities are high and the flow contains shock waves, measurements are confined to the use of a pitot tube having an external diameter of about 0.46 mm and a diameter of the sensing tube of about 0.25 mm. Total pressure measurements are made across the entire jet at several downstream locations. A survey of the sound field is conducted by using a Bruël and Kjaer 1.27-cm-diam microphone. The microphone, at a fixed position, is located about 100 diam away from the jet axis and oriented normal to the jet stream. In the present experiment, spectral measurements were not made.

The controlling parameter in this investigation is the stagnation pressure p_0, which varied for 28–74 psia, and is maintained with an accuracy of ± 0.02 psia. This range corresponds to nozzle pressure ratios (stagnation pressure/ambient pressure) varying from 1.9 to 5. An electric heater is used to keep the temperature in the settling chamber constant, usually at room temperature, to an accuracy of about 0.5°C over the duration of each test. Experiments are conducted for a number of pressure ratios using both nozzles, however, only a limited selection is presented here.

Results and Discussion

Typical shadowgraph pictures of the jet at a pressure ratio of 4.4 are shown in Fig. 1. The photographs cover the jet from the nozzle exit to a downstream distance of about 11 diam. Figure 1a corresponds to the flow from a plain or base nozzle. Typical shock cell structure with a standing normal shock wave terminated with a triple shock structure can be seen clearly in this photograph. The normal shock wave is located at about 1.45 diam from the nozzle exit. Figures 1b and 1c show the two views of the jet exiting from the slotted nozzle. The main observations from these pictures are the absence of the normal shock wave and its associate structure and the rapid spreading of the jet near the nozzle exit. Further downstream, the flow is similar to the flow from the plain nozzle with somewhat slower spreading of the jet. Large-scale vorti-

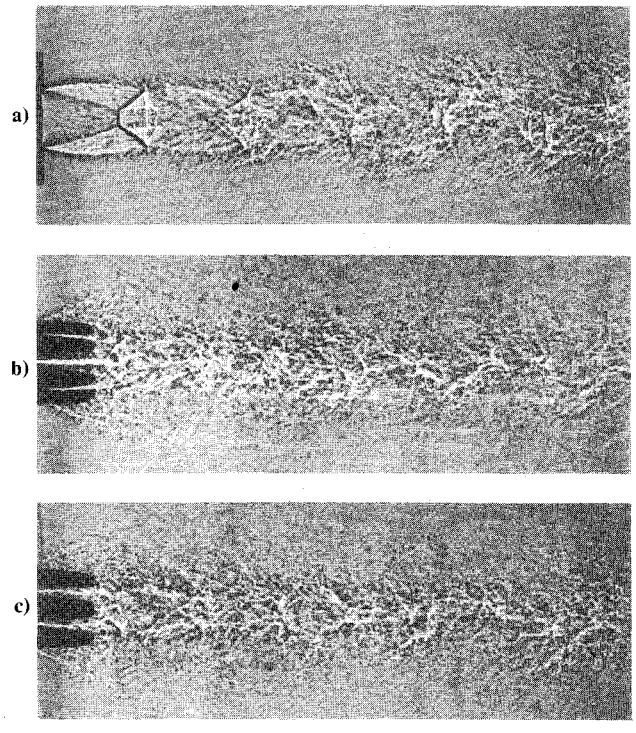

Fig. 1 Typical shadowgraph pictures of the jet at a pressure ratio of 4.4: a) plain jet; b) and c) slotted jet.

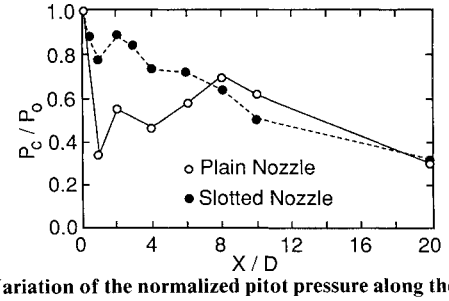

Fig. 2 Variation of the normalized pitot pressure along the centerline of the jet; pressure ratio = 4.4.

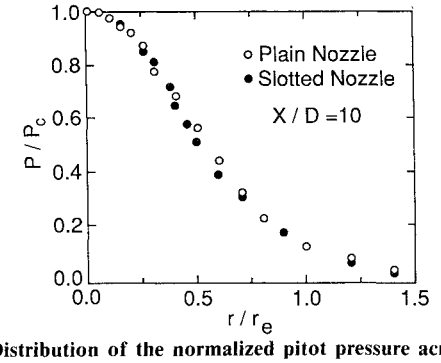

Fig. 3 Distribution of the normalized pitot pressure across the jet; pressure ratio = 4.4.

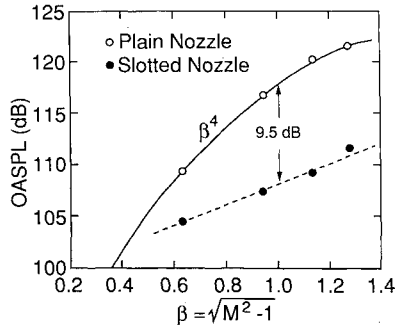

Fig. 4 The variation of the OASPL with parameter β; measurements are made at 90 deg to the jet axis.

cal structures commonly observed in axisymmetric jets can be seen from these photographs and are indicated by the arrows. For downstream locations of $X/D > 5$, these large structures are not destroyed by the presence of the slots.

A typical variation of the pitot presure P_c along the centerline of the jet for a pressure ratio of 4.4 is shown in Fig. 2. The absolute values of P_c are divided by the stagnation pressure P_0 and plotted against the nondimensionalized downstream distance. These results cannot be converted directly into velocity or Mach number because of the unknown entropy increase that has occurred. In a steady supersonic flow with a single normal shock wave ahead of the pitot tube, a large pitot pressure corresponds to low Mach number, and vice versa. For the case of the plain nozzle, near the nozzle exit, a sharp drop in the pitot pressure followed by a rise is observed, which signifies the presence of the normal shock wave commonly known as the Mach disc. For $X/D > 8$, the total pressure decays monotonically and has a variation similar to a subsonic jet. The variation of the total pressure along the centerline of the jet exiting from a slotted nozzle suggests that the shock cell structure is significantly weakened by the presence of the slots. Similar conclusions are reached from observations of total pressure profiles taken across the jet at different downstream locations.[5]

Figure 3 shows the distribution of the pitot pressure across the jet in the central plane at $X/D = 10$ and for both plain and slotted nozzles. This downstream location is well beyond the shock cell region of the jet. The pressure is normalized with respect to the centerline pressure P_c, and the distance r is normalized with the exit radius of the nozzle. It appears that both profiles have similar distribution. These and other measurements (see Ref. 5) taken at different downstream locations suggest that for $X/D \geq 10$ the influence of the fingers on the overall structure of the jet seems to be negligible. However, because of the difference in the magnitudes of the centerline pressures (see Fig. 2), the overall thrust obtained by integrating the pressure across the jet indicates that some thrust loss may occur due to the presence of the fingers or slots.

The effect of the slotting on the far-field noise can be seen in Fig. 4, which is a plot of overall sound pressure level (OASPL) against the parameter $\beta(=\sqrt{M^2 - 1})$, where M is the exit Mach number assuming an ideally expanded jet near the nozzle exit. These measurements are made at $\theta = 90$ deg and at 100 diam from the jet axis. In the case of the jet exiting from the plain nozzle, the measured levels are directly proportional to the fourth power of β, an observation consistent with other investigations. As pointed out by Harper-Bourne and Fisher,[6] the β^4 dependence indicates the dominant contribution of the shock-associated noise to the OASPL. However, measurements made with the slotted nozzle do not follow this trend, and a significant reduction in the OASPL is observed as shown in the figure. Based on the flow visualization pictures and the previous observation, it may be suggested that the reduction in the magnitude of the OASPL is due primarily to the absence of the screech tones and significantly reduced shock-associated broadband noise.

Conclusions

From these preliminary experiments, it appears that the addition of fingers or slots to a converging axisymmetric nozzle contributes to a significant noise reduction. The slots perform as silencers because they weaken the shock cell structure near the nozzle exit and thereby reduce the shock-associated noise. These slots also help to enhance the mixing close to the nozzle exit ($X/D < 10$). The present study is preliminary in nature and all implications of the results presented are not yet fully understood. Further detailed investigations are clearly needed to clarify the importance of the flow details at the nozzle exit and the flow structure close to it.

Acknowledgment

This work was carried out at Stanford University during 1978 in the Department of Aeronautics and Astronautics.

References

[1]Powell, A., "The Noise Emanating from a Two-Dimensional Jet Above the Critical Pressure," *Aeronautical Quarterly*, Vol. 4, Feb. 1953, pp. 103–122.

[2]Yu, J. C., and Seiner, J. M., "Nearfield Observations of Tones Generated From Supersonic Jet Flows," AIAA Paper 83-0706, April 1983.

[3]Glass, D. R., "Effects of Acoustic Feedback on the Spread and Decay of Supersonic Jets," *AIAA Journal*, Vol. 6, 1968, pp. 1890–1897.

[4]Krothapalli, A., Baganoff, D., and Hsia, Y., "On the Mechanism of Screech Tone Generation in Underexpanded Rectangular Jets," AIAA Paper 83-0727, April 1983.

[5]Krothapalli, A., McDaniel, J. C., and Baganoff, D., "Effects of Slotting on the Mixing and Noise of an Axisymmetric Supersonic Jet," AIAA Paper 89-1052, April 1989.

[6]Harper-Bourne, M., and Fisher, M. J., "The Noise From Shock Waves in Supersonic Jets," AGARD CP-131, 1974, pp. 11-1–11-13.

Nonlinear Analysis of an Adhesive-Bonded Joint Under Generalized In-Plane Loading

Steven G. Russell*
Northrop Corporation, Hawthorne, California 90205

Nomenclature

A^i_{mn}, A^o_{mn}	= adherend extension stiffnesses (m,n = 1 or 2)
a,b	= bond dimensions
G_c	= initial slope of the adhesive stress strain curve
G_s	= adhesive secant modulus
S_{12}, S_{21}	= uniformly distributed resultant in-plane shear loads

Presented as Paper 89-1232 at the AIAA/ASME/ASCE/AHS/ASC 30th Structures, Structural Dynamics, and Materials Conference, Mobile, AL, April 3–5, 1989; received Aug. 11, 1989; revision received and accepted for publication Jan. 23, 1990.

*Senior Engineer, Strength and Life Assurance Research, Aircraft Division. Member AIAA.